

Sudden drawdown and drainage of a horizontal aquifer

J.-Y. Parlange,¹ F. Stagnitti,² A. Heilig,¹ J. Szilagyi,³ M. B. Parlange,⁴
T. S. Steenhuis,¹ W. L. Hogarth,⁵ D. A. Barry,⁶ and L. Li⁶

Abstract. Drainage of a saturated horizontal aquifer following a sudden drawdown is reanalyzed using the Boussinesq equation. The effect of the finite length of the aquifer is considered in detail. An analytical approximation based on a superposition principle yields a very good estimate of the outflow when compared to accurate numerical solutions. An illustration of the new analytical approach to analyze basin-scale field data is used to demonstrate possible field applications of the new solution.

1. Introduction

The recession slope analysis suggested by *Brutsaert and Nieber* [1977] is a powerful tool for determining base flow separation and aquifer parameters [*Brutsaert and Lopez*, 1998; *Szilagyi and Parlange*, 1998; *Szilagyi et al.*, 1998]. The method is fundamentally linked to the behavior of the solution of the Boussinesq equation in the absence of recharge for short and long times. If Q is the discharge from the aquifer, then for short times *Brutsaert and Lopez* [1998] showed that

$$\log \left(-\frac{dQ}{dt} \right) = 3 \log Q + \log A_1 \quad (1)$$

and for long times

$$\log \left(-\frac{dQ}{dt} \right) = \frac{3}{2} \log Q + \log A_2. \quad (2)$$

The constants A_1 and A_2 are given by *Brutsaert and Lopez* [1998]:

$$A_1 = 1.1334/(kfD^3L^2) \quad (3)$$

$$A_2 = 4.8038k^{1/2}L/(fA^{3/2}), \quad (4)$$

where f is the average drainable porosity (or specific yield), k is the average hydraulic conductivity, D is the average depth of the aquifer before drainage starts, L is the length of river channels, and A is the drainage area. *Brutsaert and Lopez* [1998] also noticed that, in practice, for longer times the 3/2 slope in (2) can further decrease to about 1. The value of 3/2 corresponds to the behavior of the solution of the nonlinear Boussinesq equation, whereas the value of 1 corresponds to the behavior of the linearized equation. We shall present a

unifying theory that explains both long-term and short-term behavior. In doing so, we shall also illustrate how useful the approach is in determining effective basin-scale properties.

2. Model

Following *Brutsaert and Lopez's* [1998] notations, we consider a horizontal aquifer, with the free surface elevation given by $h(x, t)$

$$f \frac{\partial h}{\partial t} = k \frac{\partial}{\partial x} \left[h \frac{\partial h}{\partial x} \right]. \quad (5)$$

Equation (5) is to be solved with the following initial and boundary conditions:

$$h = D, \quad 0 < x < B, \quad t < 0 \quad (6)$$

$$h = 0, \quad x = 0, \quad t \geq 0 \quad (7)$$

$$\partial h / \partial x = 0, \quad x = B, \quad t > 0. \quad (8)$$

where B is the average breadth of the aquifer, so that the drainage area $A = 2BL$ for both sides of the channel.

In the limit of $B \rightarrow \infty$ or in the short time limit for B finite, the outflow Q is given by [*Polubarinova-Kochina*, 1962]

$$Q = \frac{kAD^2}{B^2} Q^*, \quad Q^* = \alpha / \sqrt{t^*}, \quad (9)$$

where Q^* is the dimensionless discharge. Note that in that case Q is proportional to $L = A/2B$;

$$t^* = Dkt/fB^2. \quad (10)$$

The standard value of the dimensionless α [*Polubarinova-Kochina*, 1962, p. 507] is

$$\alpha = 0.33206. \quad (11)$$

For this particular case the very general method of weighted residuals also yields the first three decimals correctly [*Lockington*, 1997], but the most accurate result can be found using the analogy between the Blasius and Boussinesq equations [*Polubarinova-Kochina*, 1962; *Heaslet and Alksne*, 1961] yielding [*Parlange et al.*, 1981]

$$\alpha = 0.33205734 \quad (12)$$

or, to the fourth decimal place,

$$A_1 = 1.1337/(kfD^3L^2), \quad (13)$$

¹Department of Agricultural and Biological Engineering, Cornell University, Ithaca, New York.

²School of Ecology and Environment, Deakin University, Warrnambool, Victoria, Australia.

³Conservation and Survey Division, Institute of Agricultural and Natural Resources, University of Nebraska, Lincoln, Nebraska.

⁴Department of Geography and Environmental Engineering, Johns Hopkins University, Baltimore, Maryland.

⁵Faculty of Environmental Science, Griffith University, Nathan, Queensland, Australia.

⁶School of Civil and Environmental Engineering, University of Edinburgh, Edinburgh, Scotland, United Kingdom.

Copyright 2001 by the American Geophysical Union.

Paper number 2000WR000189.
0043-1397/01/2000WR000189\$09.00

which is nearly identical to A_1 in (3).

To obtain the cumulative dimensionless outflow or volume

$$I^* = \int_0^{t^*} Q^*(\tau) d\tau, \tag{14}$$

one can solve the Boussinesq equation by linearization of the right-hand side of (5) around $h = pD$, where p is some dimensionless number, obtaining the well-known result [Brutsaert, 1994] for $B \rightarrow \infty$,

$$I^* = 1 - \frac{8}{\pi^2} \sum_{n=1}^{\infty} \frac{1}{(2n-1)^2} \exp\left[-(2n-1)^2 \frac{\pi^2}{4} p t^*\right]. \tag{15}$$

In particular, for $t^* \rightarrow 0$ this yields

$$\alpha = \sqrt{p/\pi}, \tag{16}$$

which by comparison with (12) gives a value of $p_0 \approx 1/2.887$ [Brutsaert and Lopez, 1998]. This value is close to the value $p \approx 1/3$ suggested by Brutsaert [1994], who pointed out that p should decrease with time from the largest value p_0 . The effect of the finite length, B , of the aquifer on I^* is now estimated.

3. Analytical Approximation

To estimate the effect of the finite length of the aquifer, we consider the profile for $x \sim B$. Until h falls to somewhat below D everywhere, (9) will hold. It is then logical to calculate the correction to (9) through linearization of the Boussinesq equation using the depth for $x \sim B$ which is the position where it is closer to D . Then the solution for $x \leq B$ is obtained by superposition of the semi-infinite solution for $x \leq B$ and the correction. In order to satisfy condition (8), the latter can be obtained as usual by taking the mirror image of the semi-infinite solution valid for $x \geq B$ into the region $x \leq B$, the value of the correction at $x = 2B$ having value μ to be determined later. This gives a correction to the profile h/D as the standard solution of the linear diffusion equation $\mu \operatorname{erfc} [(-2 + x/B)/\sqrt{4t^*}]$ [Carslaw and Jaeger, 1959]. Then the correction to the flux, at $x = 0$, is $[\mu/\sqrt{\pi t^*}] \exp(-1/t^*)$ or by integration in time is

$$I^* \approx 2\alpha \sqrt{t^*} - \frac{\mu}{\sqrt{\pi}} \int_0^{t^*} \frac{e^{-(1/\tau)} d\tau}{\sqrt{\tau}}, \tag{17}$$

which yields

$$I^* \approx 2\alpha \sqrt{t^*} - \frac{2\mu}{\sqrt{\pi}} \left[\sqrt{t^*} e^{-(1/t^*)} - \sqrt{\pi} \operatorname{erfc} \frac{1}{\sqrt{t^*}} \right]. \tag{18}$$

In agreement with (15), $I^* \rightarrow 1$ when $t^* \rightarrow \infty$; thus the first two terms in (18) must cancel out. Hence it must be true that

$$\mu \approx \alpha \sqrt{\pi}. \tag{19}$$

The approach can be further improved by replacing $h \sim D$ by the better approximation $h \sim D(1 - \mu \operatorname{erfc} - 1/\sqrt{t^*})$ to calculate the flux, that is, using an iterative procedure; in this case, (18) may be expressed as

$$I^* = 2\alpha \sqrt{t^*} - \frac{2\mu}{\sqrt{\pi}} \left[\sqrt{t^*} e^{-(1/t^*)} - \sqrt{\pi} \operatorname{erfc} \frac{1}{\sqrt{t^*}} \right] - \frac{\mu^2}{2} \left[\operatorname{erfc} \frac{1}{\sqrt{t^*}} \right]^2, \tag{20}$$

clearly adding correction terms to I^* which involve a higher power of $[\operatorname{erfc} 1/\sqrt{t^*}]$. Thus we express the solution by a series expansion of the form

$$I^* = 2\alpha \sqrt{t^*} [1 - e^{-(1/t^*)}] + \sum_{n=1}^{\infty} \mu_n \left[\operatorname{erfc} \frac{1}{\sqrt{t^*}} \right]^n \tag{21}$$

In (21), I^* automatically satisfies the condition $I^* \approx 2\alpha\sqrt{t^*}$ as $t^* \rightarrow 0$. As $t^* \rightarrow \infty$, the first right-hand term disappears because of the $[1 - \exp(-1/t^*)]$ term. As time increases, (2) shows that $Q \approx t^{-2}(2/A_2)^2$, and since $I^*(\infty) = 1$, I^* for large times must behave like $1 + (2Lk^{1/2}/A_2 f A^{3/2})^2/t^*$, which, in turn, must be identical with the expansion of (21) for long times. Thus three conditions result for the terms in t^{*0} , $t^{*-1/2}$ (which must be zero), and t^{*-1} . These provide three conditions to calculate the coefficients μ_n appearing in the series of (21). Thus we start anew with (21) and truncate the series after three terms since we have three conditions or

$$I^* = 2\alpha \sqrt{t^*} [1 - e^{-(1/t^*)}] + \mu_1 \operatorname{erfc} \frac{1}{\sqrt{t^*}} + \mu_2 \left[\operatorname{erfc} \frac{1}{\sqrt{t^*}} \right]^2 + \mu_3 \left[\operatorname{erfc} \frac{1}{\sqrt{t^*}} \right]^3. \tag{22}$$

There is no difficulty in calculating μ_1 , μ_2 , and μ_3 , but it is slightly simpler to use the equivalent but more compact expression

$$I^* = 2\alpha \sqrt{t^*} [1 - e^{-(1/t^*)}] + \lambda_1 \operatorname{erfc} \frac{1}{\sqrt{t^*}} + \lambda_2 \left[\operatorname{erfc} \frac{1}{\sqrt{t^*}} \right]^\nu, \tag{23}$$

where the three coefficients are now λ_1 , λ_2 , and ν . The last term in (23) replaces the last two terms in (22) so that we expect ν to be between 2 and 3. The three conditions as $t^* \rightarrow \infty$ yield

$$\lambda_1 + \lambda_2 = 1 \tag{24}$$

$$\alpha \sqrt{\pi} = \lambda_1 + \nu \lambda_2 \tag{25}$$

$$-\frac{12}{B_1^3} = \frac{2}{\pi} \lambda_2 \nu (\nu - 1), \tag{26}$$

with B_1 as the beta function, $B(\frac{2}{3}, \frac{1}{2})$ [Polubarinova-Kochina, 1962]. The result can be written very simply as

$$\nu = \sqrt{7}, \quad \lambda_1 = \frac{5}{4}, \quad \lambda_2 = -\frac{1}{4}, \tag{27}$$

which are correct to the fifth decimal place. Using these values, the α parameter may be calculated as

$$\alpha = (5 - \sqrt{7})/4 \sqrt{\pi} = 0.3320606, \tag{28}$$

which is also correct to the fifth decimal place. These yield a slightly more accurate value for A_2 than the one given in (4),

$$A_2 = 4.8050 k^{1/2} L / (f A^{3/2}), \tag{29}$$

4.8050 being the numerical value of $8[\pi/2\nu(\nu-1)]^{1/2}$.

4. Numerical Validation

Equations (23) and (27) require a truncation of the series in (21) that incorporates error in the approximation. Since (23)

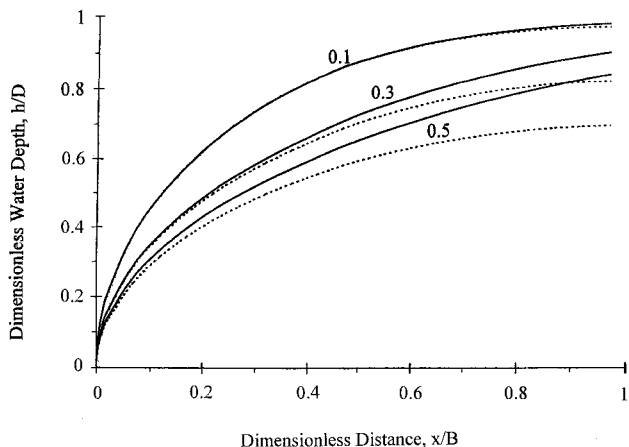


Figure 1. Water depth as a function of the dimensionless distance at various dimensionless times, showing the influence of the finite breadth of the aquifer. The results, given by the solid curves, are exact for a semi-infinite aquifer [Hogarth and Parlange, 1999], and the dotted curves represent the present numerical results for the finite aquifer.

with (27) approaches exact results in the short and long time limits, the interpolation will have maximum error at intermediate times.

The problem posed in (5)–(8) was solved numerically using a finite element program written with the aid of PDE2D, a general purpose partial differential equation solver [Sewell, 1993]. PDE2D uses a second-order accurate backward Euler scheme with an adaptive time step for transient solutions. To check the accuracy of the numerical solution, the cumulative outflow from the aquifer (I^*) was calculated as the integral (with respect to time) of the calculated discharge at $x \rightarrow 0$ as well as the integral of the depth of water (with respect to distance) at different times. Only when these two solutions were in less than 0.1% error was the numerical solution approved.

Because of the sudden, i.e., discontinuous, drawdown at $t = 0$ the numerical solution will be the least accurate as $t^* \rightarrow 0$. Thus we require the numerical solution to agree in that limit with the exact result within 10^{-5} so that the expected larger error at intermediate times will be reliably estimated. We obtain a further check of the agreement between the profiles either in the short time limit or when $B \rightarrow \infty$, for which exact results are available [Hogarth and Parlange, 1999]. Figure 1 shows that those profiles go to the right limit as $t^* \rightarrow 0$. Figure 1 also shows the increasing differences at $x \sim B$ between the finite and the semi-infinite profiles as time increases. Being confident in the numerical accuracy of the cumulative outflow when B is finite, i.e., at least to the fifth decimal place, the relative error of the analytical result given in (23), or (30) below, is indicated in Figure 2. As expected, the maximum error is for $t^* \sim 1$ and is relatively small, less than 0.4%. Substituting the coefficients from (27) into the analytical interpolation (23), we obtain the final theoretical approximation

$$I^* = \frac{5 - \sqrt{7}}{2\sqrt{\pi}} \sqrt{t^*} [1 - \exp(-1/t^*)] + \frac{5}{4} \operatorname{erfc}(1/\sqrt{t^*}) - \frac{1}{4} [\operatorname{erfc}(1/\sqrt{t^*})] \sqrt{7}. \tag{30}$$

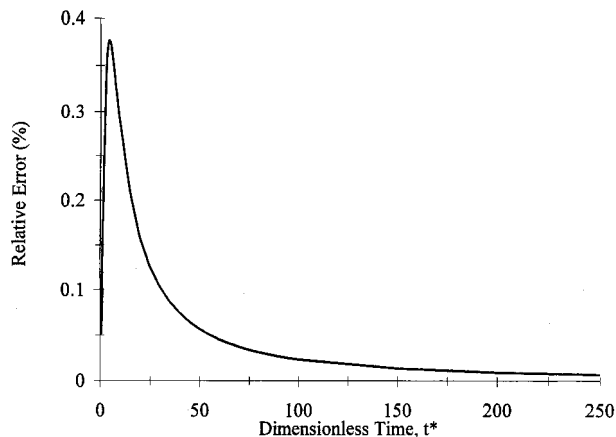


Figure 2. Relative error of the analytical solution for a finite aquifer given by equation (30) when compared to the numerical result. The maximum error of 0.38% was at $t^* \approx 4$.

5. Discussion

Following the approach of Brutsaert and Lopez [1998] in analyzing data, it is convenient to plot dQ^*/dt^* versus Q^* on a log-log scale (see Figure 3). In Figure 3 a very abrupt transition in slope is observed as it is in the field [Brutsaert and Lopez, 1998]; it is a consequence of the solution in Figure 1, in which the profile is first affected by the finite width of the aquifer, around time $t^* = 0.1$. However (Figure 4), the cumulative outflow does not reflect the effect of the finite length until after $t^* \approx 0.6$; hence the profiles near $x = 0$ and the outflow at $x = 0$ are not affected for a relatively long time. This is because, according to the Boussinesq model, diffusion is small where h is small, i.e., for $x \approx 0$. For $x \approx B$ where diffusion is the largest (highest head), the profiles are flatter than for the semi-infinite profiles, but this does not rapidly influence the region where h is small. Thus by the time the flux at the outflow is significantly reduced, h at $x \approx B$ has about half its initial value.

The present model predicts a 1.5 slope for long times in Figure 3 and not a slope of 1 as sometimes observed. One can speculate as to possible causes for a slope of 1. Here we

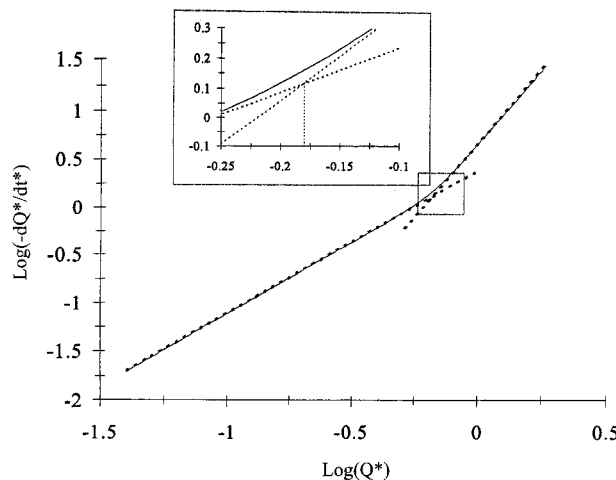


Figure 3. Plot of dQ^*/dt^* versus Q^* on a log-log scale from the analytical result of equation (30).

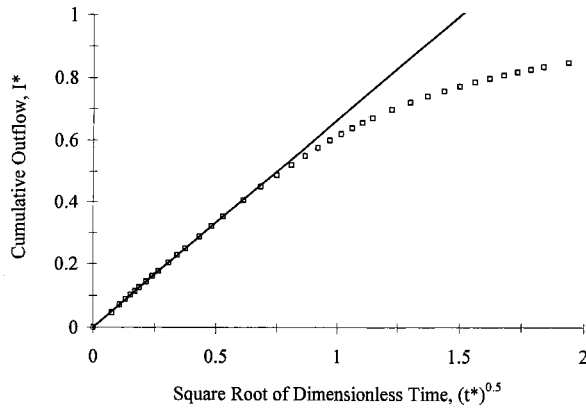


Figure 4. Dimensionless cumulative outflow plotted with dimensionless square root of time. The straight curve is the exact result for a semi-infinite aquifer. The squares show the numerical result for a finite aquifer. The two deviate from each other for long times.

consider the case when Darcy's law and Boussinesq's equation dominate, but when the flow is greatly reduced, many local features, for example, small ponds, might contribute to water movement which are neglected when h is large. The addition of all those small independent mechanisms are typical of random behavior, leading to linear diffusion and hence a slope of 1. The same effect would also result if a full drawdown did not take place; then after a long time, linear diffusion takes place providing again a limiting slope of 1 for long times. This does not invalidate the use of Figure 3 for field data as long as the transition to the 1.5 slope takes place before the slope of 1 occurs.

6. Field Data Analysis

This section provides an illustration of a possible method to analyze data to obtain catchment properties using (30). Field data were obtained from East Mahantango Creek near Dalmatia, Pennsylvania, station 01555500, a tributary of the Susquehanna River in the nonglaciated part of the North Appalachian Ridge and Valley Region, U.S. Geological Survey National Water Information System. The catchment is characterized by Devonian sandstone, siltstone, and shale underlying thin moderately weathered channery or stony loam soils with poorly developed horizons. The catchment area is 423 km² with a drainage density of 0.68 km⁻¹. Annual precipitation is around 1 m. The catchment is heavily forested; more than 70% of its drainage area is woodland.

Figure 5 shows recession flow data (daily mean runoff) for the Mahantango Creek, Pennsylvania, watershed (1984–1987) 1 day after precipitation ceased. The dQ^*/dt^* and Q^* data can be superimposed onto the curve of Figure 3 with a translation equal to $\log(kAD^2B^{-2})$ in the horizontal direction and equal to $\log(Ak^2D^3f^{-1}B^{-4})$ in the vertical direction. Following this procedure, (30) was fitted directly to all the points in Figure 5 by nonlinear regression with horizontal $\log H$ and vertical $\log V$ translation. For this average curve we find $H = 1/0.036$ and $V = 1/22,000$ with an $r^2 = 0.68$.

We are making no attempt at a proper statistical analysis of the field data, as this is not the purpose of this paper. Rather we want to fit different curves to the data to illustrate the

sensitivity of the results to the choice of the curve. For instance, we could use the lower envelope of the data [Brutsaert and Lopez, 1998]. Instead, we generate an upper and lower curve with the following recipe: Fifteen intervals were chosen with constant ΔQ increments. The data points were averaged to calculate the arithmetic mean values of dQ/dt in each interval, and (30) was again fitted to these 15 points; by this artificial procedure, $r^2 = 0.96$ is naturally very high. This procedure, for example, with 15 intervals, was chosen as it led to the same values of H and V as obtained previously with all data points. Then 95% confidence intervals on those 15 points were used to obtain the upper and lower curves in Figure 5, using (30). Again those curves do not give a proper representation of the uncertainty of the data but provide an illustration of the sensitivity of the results to the choice of the curve fitting. We find for the lower curve, $H = 1/0.03$ and $V = 1/22,000$, and for the upper curve, we find $H = 1/0.035$ and $V = 1/16,000$.

The shift parameters H and V are defined by

$$H = kAD^2B^{-2} \quad (31)$$

$$V = Ak^2D^3f^{-1}B^{-4}, \quad (32)$$

where A is the drainage area (4.23×10^8 m², $B = A/(2L)$ and L is total stream length (2.87×10^5 m).

Therefore the values for Df and kD^2 are, for the average curve, $Df = 0.0402$ and $kD^2 = 0.0357$; for the lower curve $Df = 0.0581$ and $kD^2 = 0.0429$, and the upper curve gives $Df = 0.0303$ and $kD^2 = 0.0367$. The difference between the two extreme sets of values gives some crude estimate of the sensitivity of the results. Of course, one more parameter has to be measured, for example, D or f , to predict the other two. For instance, if $f \approx 0.02$, the average, upper, and lower curves give $D \approx 2.0 \pm 0.07$ m and $k \approx 0.01 \pm 0.005$ m s⁻¹. Note that the values of k tend to be large as discussed by Brutsaert and Lopez [1998].

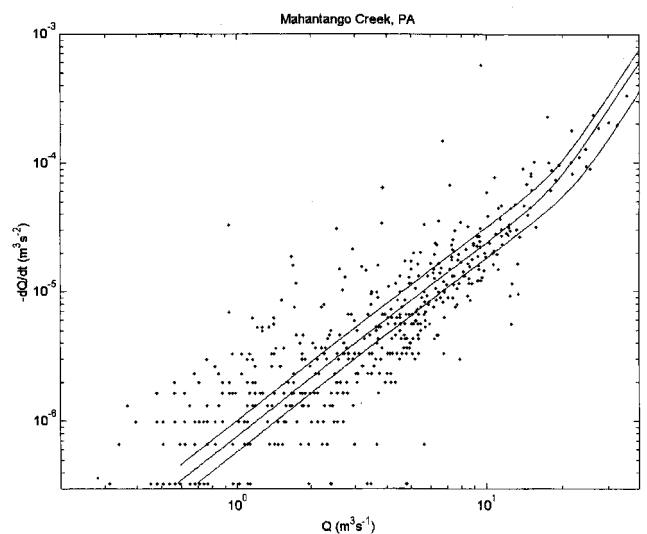


Figure 5. Illustration of the method using recession flow data for the Mahantango Creek with equation (30), showing the average fit and the 95% confidence intervals of the means for 15 intervals.

7. Conclusions

On the basis of the Boussinesq equation a new simple and accurate analytical approximate solution is obtained which is tested for error magnitude and sensitivity, and a typical data set is used to demonstrate its application to analyze basin outflow. Specifically following *Brutsaert and Lopez* [1998], a one-dimensional model is used to describe a catchment response for estimating basin-scale parameters. The model requires that the data (as plotted in Figure 3) show a slope of 3 for the short times and 1.5 for the long times. The long time behavior is less crucial when an abrupt change in slope appears at a well-defined value of Q and dQ/dt . The theory predicts this abrupt change in slope, and this knowledge can be used to obtain two relations that predict useful, effective, basin-scale properties.

Acknowledgment. The authors are grateful to W. Brutsaert of Cornell University for suggesting this topic of research and for many helpful discussions. The second author acknowledges the support of the Department of Industry, Science and Resources (Australia), International Collaboration Project (16), and OECD travel fellowship.

References

- Brutsaert, W., The unit response of groundwater outflow from a hill-slope, *Water Resour. Res.*, *30*, 2759–2764, 1994.
- Brutsaert, W., and J. P. Lopez, Basin-scale geohydrologic drought flow features of riparian aquifers in the southern great plains, *Water Resour. Res.*, *34*, 233–240, 1998.
- Brutsaert, W., and J. L. Nieber, Regionalized drought flow hydrographs from a mature glaciated plateau, *Water Resour. Res.*, *13*, 637–643, 1977.
- Carslaw, H. S., and J. C. Jaeger, *Conduction of Heat in Soils*, 2nd ed., Oxford Univ. Press, New York, 1959.
- Heaslet, M. A., and A. Alksne, Diffusion from a fixed surface with a concentration-dependent coefficient, *J. Soc. Ind. Appl. Math.*, *9*, 584–596, 1961.
- Hogarth, W. L., and J.-Y. Parlange, Solving the Boussinesq equation using solutions of the Blasius equation, *Water Resour. Res.*, *35*, 885–888, 1999.
- Lockington, D. A., Response of an unconfined aquifer to sudden change in boundary head, *J. Irrig. Drain. Eng.*, *123*, 24–27, 1997.
- Parlange, J.-Y., R. D. Braddock, and G. Sander, Analytical approximation to the solution of the Blasius equation, *Acta Mech.*, *38*, 119–125, 1981.
- Polubarinova-Kochina, P. Y.-A., Theory of groundwater movement, translated from Russian by R. J. M. DeWiest, 613 pp., Princeton Univ. Press, Princeton, N. J., 1962.
- Sewell, G., PDE2D: Easy to use software for general two-dimensional partial differential equations, *Adv. Eng. Software*, *17*, 105–112, 1993.
- Szilagy, J., and M. B. Parlange, Base flow separation based on an analytical solution of the Boussinesq equation, *J. Hydrol.*, *204*, 251–260, 1998.
- Szilagy, J., M. B. Parlange, and J. D. Albertson, Recession flow analysis for aquifer parameter determination, *Water Resour. Res.*, *34*, 1851–1858, 1998.
- D. A. Barry and L. Li, School of Civil and Environmental Engineering, University of Edinburgh, Edinburgh EH9 3JN, Scotland, UK. (A.Barry@ed.ac.uk; Ling.Li@ed.ac.uk)
- A. Heilig, J.-Y. Parlange, and T. S. Steenhuis, Department of Agricultural and Biological Engineering, Riley-Robb Hall, Cornell University, Ithaca, NY 14853. (arik@engr.uconn.edu; jp58@cornell.edu; tss1@cornell.edu)
- W. L. Hogarth, Faculty of Environmental Science, Giffith University, Nathan, Queensland 4111, Australia. (b.hogarth@ens.edu.au)
- M. B. Parlange, Department of Geography and Environmental Engineering, Ames Hall, Johns Hopkins University, Baltimore, MD 21218. (mbparlange@jhu.edu)
- F. Stagnitti, School of Ecology and Environment, Deakin University, Warrnambool, Victoria 3280, Australia. (frankst@deakin.edu.au)
- J. Szilagy, Conservation and Survey Division, Institute of Agricultural and Natural Resources, University of Nebraska, Lincoln, NE 68588. (jszilagy@unlinfo.unl.edu)

(Received June 19, 2000; revised November 10, 2000; accepted March 8, 2001.)

